

# Application of magnetic fabric studies in an ancient fluvial sequence of NW Himalaya

S. J. Sangode\*, Rohtash Kumar and Sumit K. Ghosh

Wadia Institute of Himalayan Geology, Dehra Dun 248 001, India

**We report here an account of sedimentary magnetic fabrics in 44 channel sand-bodies of a Siwalik fluvial sequence (6 to 0.5 Ma) near Nahan, Himachal Pradesh. These sandstones in distal alluvial fan-setting record oblate fabrics ( $T_{\text{mean}} = 0.51$ ) and relatively higher degree of anisotropy ( $Pj_{\text{mean}} = 1.05$ ). The minimum axis ( $K3$ ) of the anisotropy ellipsoid is aligned parallel to the palaeoflow direction by traction carpet mechanism. Variations with time of latitudes derived from azimuth of principle ellipsoid axes show a greater sensitivity to the basin tectonic impulses with smaller response time than conventional methods. This signifies the scope of magnetic fabric techniques for palaeo-hydrodynamic and basin tectonic studies in the Indo-Gangetic foreland of Himalaya.**

MAGNETIC fabrics in the form of magnitude, shape and orientation of ellipsoids are becoming increasingly important for strain determinations in weakly-deformed rocks<sup>1</sup>. Recently this technique has also been proved equally useful in the investigation of flow-related parameters (e.g. palaeocurrent direction and intensity) that are controlled by primary/depositional fabrics<sup>2</sup>. Previously, Sangode *et al.*<sup>3</sup> made use of magnetic fabrics in Siwalik sediments to infer the turbulence due to tectonic impulse or climate dynamics that envisage its scope in flood-related studies. Thus we investigate in detail the magnetic fabric characteristics in the channel sands of the Upper Siwalik sediments in Indo-Gangetic foreland basin (IGFB, Figure 1) using a more sophisticated equipment.

The IGFB is a peripheral foreland basin where the northern belt is folded, thrust and uplifted representing the Outer/Sub Himalaya currently undergoing erosion by antecedent rivers<sup>4</sup>. In the southern part of the IGFB, active sedimentation in the form of alluvial fans is taking place. Sedimentological aspects in the IGFB are detailed in Singh<sup>4</sup>, Burbank *et al.*<sup>5</sup>, Tandon<sup>6</sup> and Parkash *et al.*<sup>7</sup>.

Earlier Sangode *et al.*<sup>3</sup> reported magnitude- and shape-related parameters of the anisotropy of magnetic susceptibility (AMS) in this area by modification of sample insertion system of Bartington's Magnetic Susceptibility meter (MS-2B). We present here a range of the AMS parameters (directional, magnitude- and shape-related)

using a sensitive version of KLY-3S spinner kappabridge anisotropy meter of AGICO (Czech Republic) to investigate its scope in the IGFB and its basin tectonic responses due to Himalayan upliftments.

## Approach

The Haripur section in Nahan area was dated to be 6 to 0.5 Ma by magnetic polarity stratigraphy<sup>8</sup>. Detailed investigation using biostratigraphy, palynostratigraphy and sedimentology for the studied section was carried out by Nanda *et al.*<sup>9</sup>, Phadtare *et al.*<sup>10</sup> and Kumar *et al.*<sup>11</sup>, respectively. The present sampling for magnetic fabric studies was done on 44 well-defined channel sand-bodies from the Haripur section (described in Kumar *et al.*<sup>11</sup>) using a portable rock drill. The collected samples are all from hard compact layers of medium-grained sandstones without obvious local primary sedimentary structures. The cores were cut into cylindrical samples of 2.5 cm diameter and 2.2 cm length (maintaining an approximate 0.86 ratio of the length to diameter) and washed with dilute acid to remove machine contaminations. Initially each sample was measured in six directions in low and high frequencies of the applied field using Bartington's MS-2B laboratory sensor to obtain the frequency dependence of susceptibility ( $X_{fd}\%$ ), a parameter to depict the relative variation of magnetic grain-size. Further, all the anisotropy parameters were calculated by analysis in the spinner mode of KLY-3S kappabridge after calibration to standards and confirmation with the manual mode (15-direction). The magnitude of fabric ellipsoid in the form of degree of AMS ( $Pj$ ) and the shape parameter ( $T$ ) are derived from equations given by Tarling and Hrouda<sup>2</sup>. Shape of the anisotropy ellipsoid ( $T$ ) is used to infer prolate ( $-1 \leq T < 0$ ), neutral ( $T = 0$ ) and oblate ( $0 < T \leq 1$ ) fabrics<sup>2</sup>. Degree of foliation ( $F$ ) and degree of lineation ( $L$ ) were calculated using the equations of Stacey<sup>12</sup> and Balsley and Buddington<sup>13</sup>, respectively. The directions (declination and inclination) of principle susceptibility axes ( $K1 = \text{maximum}$ ,  $K2 = \text{intermediate}$  and  $K3 = \text{minimum}$ ) are calculated using a computer program, SUSAR, available with the KLY-3S kappabridge. Since the rock strata are dipping at high angles ( $> 20^\circ$ ), tilt corrections are made for each sample site. Latitudes were calculated from the direction of principle susceptibility axes using the

\*For correspondence. (e-mail: sangode@rediffmail.com)

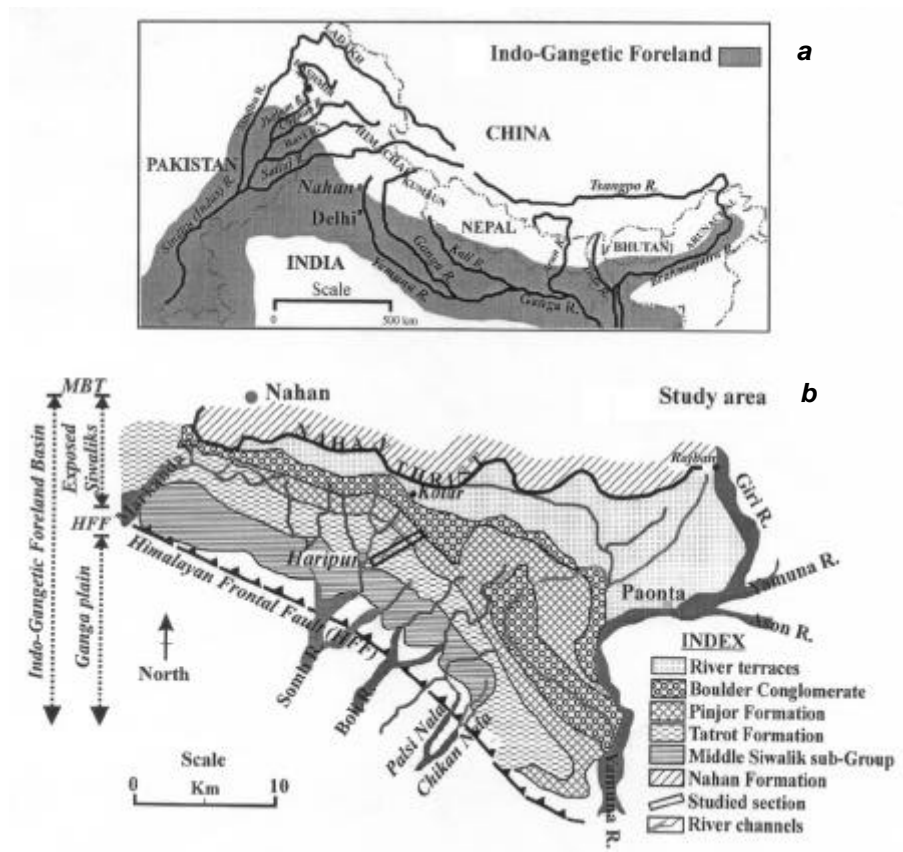


**Figure 1.** a, Geographic extent of Indo-Gangetic foreland basin (shaded) with major rivers flowing through; b, Geological map of the study area after Srivastava *et al.*<sup>17</sup> showing the studied section near Haripur. MBT, Main Boundary Thrust; HFF, Himalayan Frontal Fault.

virtual geomagnetic pole derivation given in Butler<sup>14</sup>. Coefficient for bottom-water current velocity ( $C_v$ ) was adopted from Ellwood and Ledbetter<sup>15</sup>.

## Results and discussion

The mean degree of anisotropy ( $P_j$ ) for the studied section ( $= 1.051$ , with minimum  $= 1.006$  and maximum  $= 1.14$ ) is significantly higher than earlier reports from sedimentary rocks<sup>16</sup> and tends towards anchimeta-morphism grade<sup>2</sup>. The high  $P_j$  in these sediments might have resulted from (a) enhancement due to burial compaction, and/or (b) original high anisotropy of the depositional fabrics. These sediments after deposition, have been buried to  $> 1$  km depth for over a million years. Therefore, it is important to find the effect of compaction due to burial on the magnetic fabrics. The  $K_3$  axis making high angles to the bedding plane is the most ideal parameter for such investigation. Hence we plotted the tilt corrected inclinations of  $K_3$  with depth (height of the section, Figure 2). With the linear regression line there is no observable effect of such compaction. On the contrary, the inclination increases with depth. However, when an

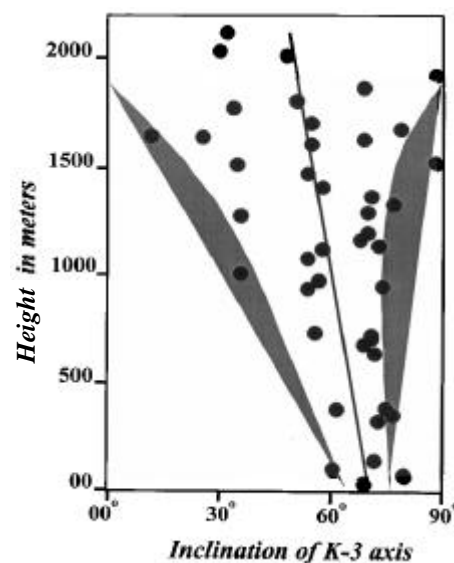


**Figure 2.** Variation of the inclination of minimum susceptibility axis- $K_3$  with stratigraphic height of the studied section to depict the depth relation of magnetic fabrics (see details in text). The inclined line represent the linear regression and the grey shaded envelope is to depict the scatter of data with height.

envelope is plotted, it is observed that the scatter converges with depth. Thus one needs to explain whether the decrease in scatter with depth is due to post-depositional effect of burial compaction or the increase in scatter with height is because of original palaeocurrent variability. The field characters (trough cross stratifications and imbrication directions) and the orientation of *K3* axis (the palaeocurrent direction discussed later) support the latter possibility of increased palaeoflow variability (direction and velocity). Yet, detailed experimental work is needed to understand the effect of burial compaction over magnetic fabrics in the Siwalik sediments.

The histogram for *Pj* shows frequency distribution with maximum frequency in the bin of 1.05 to 1.06, followed by the bins 1.02 to 1.04, and 1.1 to 1.12 (See Figure 3 *a*). Figure 3 *b* explains the change in shape of the fabrics (*T*)

with degree of anisotropy (*Pj*). Shape of the fabrics is consistent in the positive quadrant even after change in anisotropy (*Pj*), indicating dominantly oblate (disc)-shaped nature of the fabrics. Figure 3 *c* showing the effect of linearity (*L*) versus planar components of the magnetic fabric also infers a strong oblateness of fabric. The plots in Figure 3 *b* and *c* broadly distinguish the data into two major clusters separated by  $Pj \cong 1.09$  and  $F \cong 1.05$ , respectively. As described above, the histogram for *Pj* (Figure 3 *a*) has distinguished three clusters. Therefore, we classify the samples into three groups; (I)  $Pj \leq 1.05$ , (II)  $Pj = 1.05$  to 1.06, and (III)  $Pj = 1.1$  to 1.12; and the related mean parameters for each group are plotted in Figure 4. A clear relationship shown by the magnetic susceptibility ( $X_{if}(\text{mean})$ ) and the degree of anisotropy ( $Pj_{\text{mean}}$ ) is that the higher anisotropies are shown by large  $X_{if}$  samples and the  $X_{fd}\%$  indicates a relatively larger grain size in higher anisotropy groups (Groups II and III), suggesting a mineralogical control over such parameters. This suggests a need for careful assessment while dealing with the shape- and magnitude-related parameters alone (i.e. without taking into account direction and rock magnetic composition). The parameters *F*, *L* and *Cv* show almost equal distribution in all the groups.

The tilt-corrected directions using declination and inclination data for the three principle axes are plotted

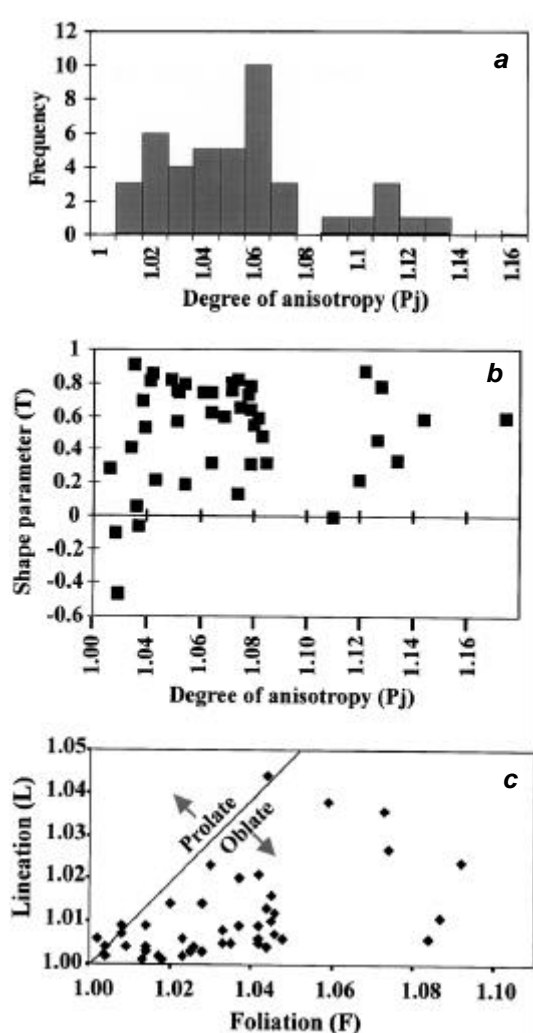


**Figure 3.** Distribution of the magnitude-related parameters of the magnetic fabrics in the studied section. *a*, Histogram for *Pj* (degree of anisotropy of magnetic susceptibility) showing the frequency on ordinate and the bins for *Pj* values on abscissa; *b*, Distribution of *Pj* versus *T* (shape parameter) indicating a dominantly oblate nature of magnetic fabrics; *c*, Magnetic lineation (*L*) versus foliation (*F*) plot also describing the oblate (disc)-shaped nature of fabrics.

	00%	50%	100%	
	8.54	7.58	31.42	$X_{if}(\text{mean})$
	3.86		15.05	$X_{if}(\text{min.})$
	.55	15.08	69.79	$X_{if}(\text{max.})$
	2.83		1.12	$X_{fd}\%$
	1.02	1.04	1.07	<i>F</i>
	1.005	1.009	1.026	<i>L</i>
	1.026	1.056	1.106	<i>Pj</i>
	0.48	0.65	0.46	<i>T</i>
	214	109	198	<b>K1-D</b>
	17	17	23	<b>K1-I</b>
	151	208	182	<b>K2-D</b>
	16	19	15	<b>K2-I</b>
	177	169	99	<b>K3-D</b>
	62	58	62	<b>K3-I</b>
	1.0302	1.061	1.1304	<i>Cv</i>
	<b>Group-I</b>	<b>Group-II</b>	<b>Group-III</b>	

**Figure 4.** Total percentage distribution of the studied parameters classified with three groups (Group-I for  $Pj < 1.05$ , Group-II for  $Pj = 1.05$  to 1.06, and Group-III for  $Pj = 1.1$  to 1.12). Numbers inside the histogram indicate the mean value for the percentage distribution in the respective group of the respective parameter (e.g. 18% of the  $X_{if}(\text{mean})$  falls in Group-I with the mean susceptibility value of 8.54 units).

separately in Figure 5. The general distribution of  $K1$ ,  $K2$  and  $K3$  axes shows oblate nature of fabrics, coinciding with other parameters discussed above. The maximum density contours (9.38, 7.81 and 6.25%) are shown by distribution of  $K3$  axes. The contour density of 9.38% trends in SW-NE direction dipping at high angles (60 to 80°) in the NE quadrant (i.e. imbrication towards SW) and is in close agreement with predominant south-westerly-flowing transverse trunk drainage system reported by Kumar *et al.*<sup>11</sup> in this section. A density of 7.81% towards south and 6.25% towards SE direction corresponds to the palaeoflow variability of secondary and

piedmont drainage system (see the comparison in Figure 6 and more details in Kumar *et al.*<sup>11</sup>). Further, the  $K1$  direction shows maximum distribution in NW-SE direction, i.e. perpendicular to the maximum distribution direction of  $K3$  in agreement with the traction carpet mechanism suggested earlier by Sangode *et al.*<sup>3</sup> in this basin.

### Palaeoflow variability

Kumar *et al.*<sup>11</sup> conducted detailed palaeoflow measurements in the studied section using 266 sets of trough cross-strata (TCS) and more than 2000 clast imbrication

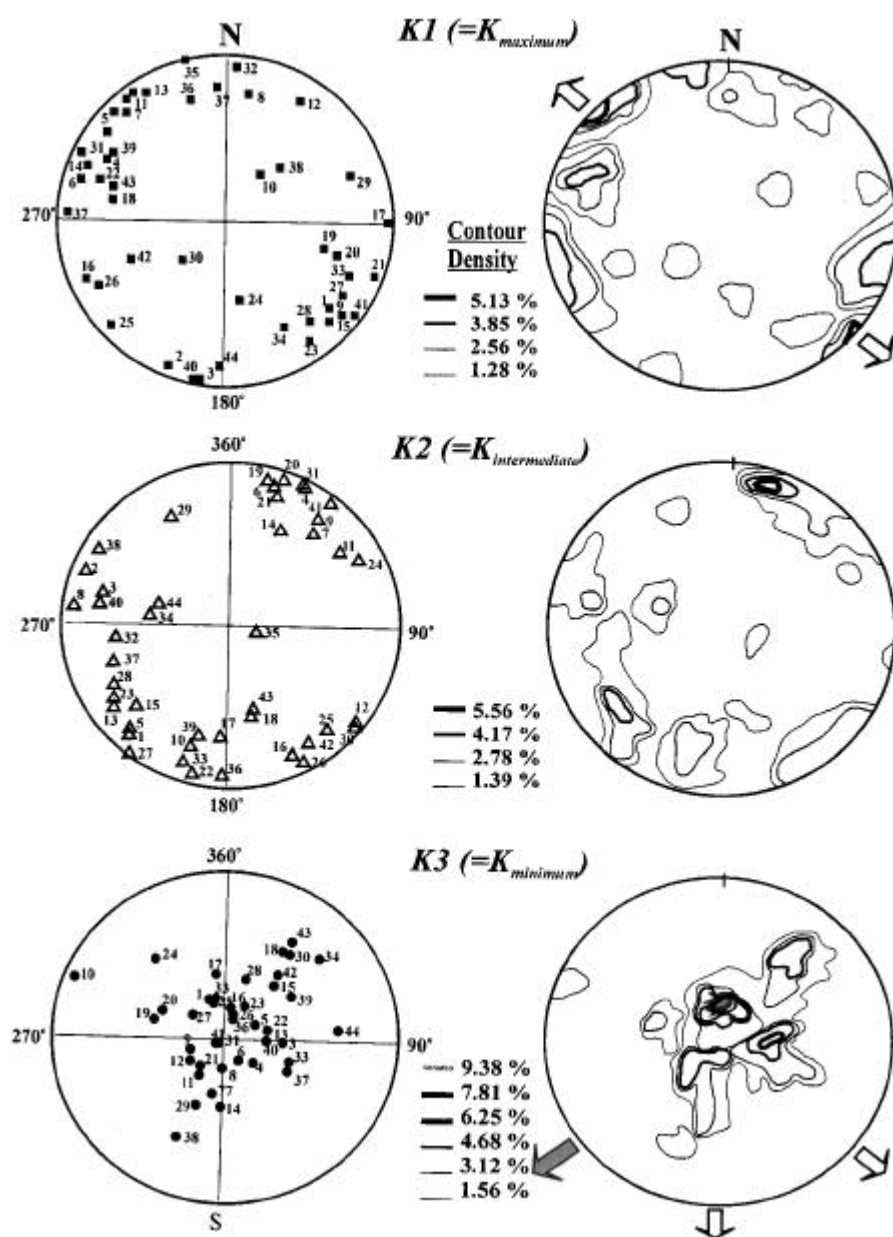


**Figure 5.** Distribution of the tilt-corrected directions of the principle susceptibility axes on equal area stereonet plot (left-hand side). Numbers alongside of each symbol indicate the site number in the studied section. Contours are drawn from the equal area distribution of  $K1$ ,  $K2$  and  $K3$  direction using Kalsbeck method (described in Marshak and Mitra<sup>18</sup>) to depict the distribution of the principle susceptibility axes and their consistency with palaeoflow (see text for details).

data. In the basal 0–400 m part, the palaeoflow is mainly towards the south-east, with a secondary mode towards the north-east. This part of the section comprises multi-storied grey-sheet sand-bodies deposited in large braided river systems comparable with the magnitude of present Ganga river<sup>11</sup>. In this part, a more realistic comparison of palaeoflow direction is shown by the *K1* axis (PC2 in Figure 6) and *K3* (PC3) is more or less scattered or follows the secondary currents. The variation in  $X_{lf}$ ,  $X_{fd}$ ,  $P_j$ ,  $T$  and  $C_v$  is relatively smooth. An inverse relation is observed for bottom-water current velocity to the magnitude of sand-bodies in the entire section. Between 400 and 1600 m, the overbank mudstones and palaeosols are also increased, while the magnitude and frequency of sandstones has decreased with higher lateral accretion and channel plug deposits<sup>11</sup> and the palaeoflow is mainly towards the south-west<sup>11</sup>. In this part,  $C_v$  stands increased with large fluctuations and the directions of *K3* show a more realistic comparison to palaeoflow (See Figures 6 and 7). At 760 m, there is an instantaneous rise in  $X_{lf}$  and  $P_j$  that post-dates the instantaneous changes in the lati-

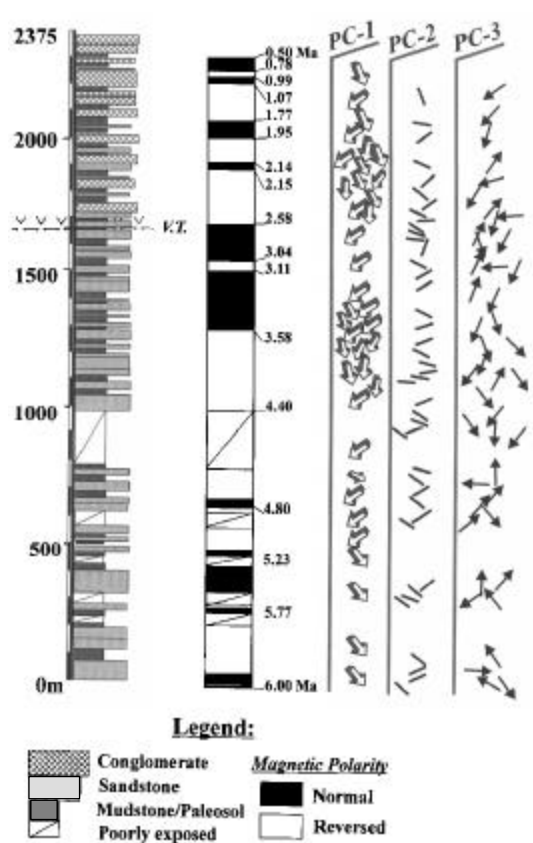


**Figure 6.** Composite litho-column (in metres) and magnetostratigraphic chronology (in million years) of the studied section (after Sangode *et al.*<sup>8</sup>) shown with palaeoflow directions derived from different sources of data. PC-1, palaeoflow directions using field data, based on trough cross-stratifications and pebble imbrications; PC-2, directions of the *K1* axes of magnetic fabrics (plotted as scalar due to shallow inclination of *K1*); and PC-3, Directions (arrows) derived from the orientation of the minimum susceptibility axis (*K3*) of the magnetic fabric ellipsoid.

tudes of *K1* and *K2* axes (See VGP-K1 and VGP-K2 at 650 m in Figure 7). The 760 m level in the studied section characteristically marks the first appearance of buff-coloured ribbon sandstone in a general occurrence of grey sand-bodies in the underlying sequence. The buff sand-bodies are associated with higher proportion of flood-plain deposits and are smaller in magnitude (compared to grey sand-bodies). It shows small-scale trough cross-strata and parallel laminations, indicating low magnitude rivers that have laterally fixed channels and piedmont drainage system. Kumar *et al.*<sup>11</sup> described the appearance of buff-coloured sandstone as widespread initiation of the piedmont drainage in the foreland due to intra-basinal tectonic activity.

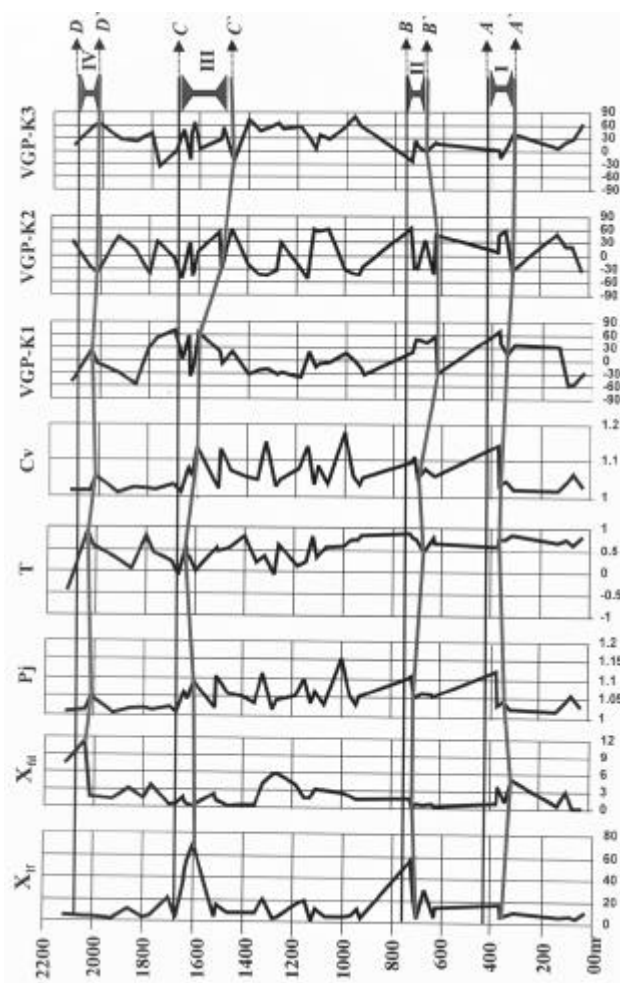


**Figure 7.** Studied magnetic parameters plotted with height of the section (in metres) describing four major basin tectonic events (Roman numbers). Black horizontal lines (indicated by bold letters A, B, C, D) record the major basin tectonic events observed from appearance of a characteristic clast or litho-facies<sup>11</sup> and the grey ‘tie lines’ mark the corresponding response to change in magnetic fabric parameters (marked by A’, B’, C’ and D’). I, Major change in lithofacies from multistoried sandstones to overbank facies with thick palaeosol deposits corresponding to a tectono-climatic change described by Sangode *et al.*<sup>3</sup>; II, First notable appearance of buff sandstone indicative of onset of the piedmont drainage in this basin; III, Pinjor/Tatrot formational boundary and occurrence of major pre-Tertiary clast-bearing conglomerates that indicate re-activation of MBT; IV, Occurrence of Tertiary clast-bearing conglomerates indicative of Nahan thrust activity<sup>3,8,11</sup>.

The peak in susceptibility ( $X_{lf}$ ) at 1600 m level corresponds to peaks in  $P_j$  and  $C_v$  and a drop in  $T$  (i.e. increased prolateness of fabrics). A major pre-Tertiary (P-T) clast-bearing sand-body appears at the 1670 m level and is followed by thick overbank deposits. Magnetostratigraphic data<sup>8</sup> precisely demarcate the Tatrot/Pinjor Formation boundary at this level and records enhanced rates of sedimentation. The conspicuous drop in  $C_v$  and  $P_j$  at 1700 m corresponds to a major change in palaeoflow directions (Figures 6 and 7) that agrees well with the basin evolutionary model of Kumar *et al.*<sup>11</sup>. There is a peak in  $X_{fd}$  at 2020 m, with increased oblateness of fabrics. This corresponds to a significant drop in rate of sedimentation<sup>8</sup> and thus suggests upliftment in this part of the basin. The first appearance of Tertiary clast-bearing conglomerate at 2100 m, that is indicative of Nahan Thrust activity<sup>11</sup>, supports the above records of upliftment.

### Response time

In an orogenic belt and foreland setting, there is a delay in signatures received in the foreland (depo-centre) of the tectonic activity at the orogenic front. As an example, the major occurrence of pre-Tertiary clast-bearing conglomerate indicative of Main Boundary Thrust (MBT) activity observed above ~1600 m level post-dates the thrusting event because of the delay due to sediment transport and progradation. On the other hand, the magnetic fabric parameters are controlled by hydrodynamic regime and thus record a lesser response time than the field observations of first appearance of characteristic clasts. Such an observation is well-exemplified in Figure 7 between the selected major inferred basin tectonic events in the Haripur section, to observe their connections with major preceding changes in the magnetic parameters (marked by horizontal lines in Figure 7). It is noted that amongst all the parameters, the VGP latitudes of  $K1$  and  $K2$  show a maximum sensitivity (or in other words the minimum response time) to the basin tectonic impulses. The change in magnetic parameters is always recorded earlier by ~50 to 100 m (see the grey tie lines in Figure 7) than the observable signatures in field<sup>11</sup> (marked by the black horizontal lines). Considering the average rate of sedimentation of 45 cm/1000 years calculated for the given section by Sangode *et al.*<sup>8</sup>, the difference of 50 to 100 m corresponds to 100 to 250 × 10<sup>3</sup> years. Hence we suggest the use of these parameters to get an improved record of tectonic events in a basin.

### Conclusions

The channel sand-bodies in the distal alluvial fan setting of the Haripur section of Upper Siwaliks in Nahan area (NW Himalaya) record oblate fabrics with relatively

higher anisotropies. The minimum susceptibility axis ( $K3$ ) is preferably aligned to the palaeoflow direction in most of the channel sands. The predominantly oblate nature of background magnetic fabric tends towards prolateness with observable tectonic signatures. The VGP latitudes derived from the orientation of the principal susceptibility axes ( $K1$  and  $K2$ ) show a response time better by 100 to 250 thousand years than the observable basin tectonic/climatic events recorded in litho-units. Thus the magnetic fabric technique indicates a wider scope of application in the IGFB and needs to be developed for its applications in the active sedimentation over the Ganga plain and the adjoining areas.

1. Borradaile, G. J. and Henry, B., *Earth Sci. Rev.*, 1997, **42**, 49–93.
2. Tarling, D. H. and Hrouda, F., *The Magnetic Anisotropy of Rocks*, Chapman and Hall, London, 1993, p. 217.
3. Sangode, S. J., Kumar, R. and Ghosh, S. K., in *The Indian Subcontinent and Gondwana: A Palaeomagnetic and Rock Magnetic Perspective* (eds Radhakrishna, T. and Piper, J. D. A.), Memoir Geol. Soc. India, 1999, vol. 44, pp. 221–248.
4. Singh, I. B., *Gondwana Res. Group Mem.*, 1999, vol. 6, pp. 247–262.
5. Burbank, D. W., Beck, R. and Mulder, T., in *Tectonic Evolution of Asia* (eds Yin, A. and Harrison, T. M.), Cambridge Univ. Press, 1996, pp. 149–188.
6. Tandon, S. K., In *Sedimentary Basins of India, Tectonic Context* (eds Tandon, S. K., Pant, C. and Casshyap, S. M.), Gyanodaya Prakashan, Nainital, 1991, pp. 171–201.
7. Parkash, B., Sharma, R. P. and Roy, A. K., *Sediment. Geol.*, 1980, **25**, 127–159.
8. Sangode, S. J., Kumar, R. and Ghosh, S. K., *J. Geol. Soc. India*, 1996, **47**, 683–704.
9. Nanda, A. C., Sati, D. C. and Mehra, G. S., *J. Himalayan Geol.*, 1991, **2**, 151–158.
10. Phadtare, N. R., Kumar, R. and Ghosh, S. K., in *Siwalik Foreland Basin of Himalaya* (eds Kumar, R., Ghosh, S. K. and Phadtare, N. R.) Sp. Pub. Himalayan Geology, 1994, vol. 15, pp. 69–82.
11. Kumar, R., Ghosh, S. K. and Sangode, S. J., *Geol. Soc. Am. Bull. Spl. Pap.*, 1999, **328**, 239–256.
12. Stacey, F. D., *Nature*, 1960, **188**, 134–135.
13. Balsley, J. R. and Buddington, A. F., *Am. J. Sci.*, 1960, **A258**, 6–20.
14. Butler, R. F., *Palaeomagnetism: Magnetic Domains to Geologic Terranes*, Blackwell Scientific Pub., Oxford, 1992, pp. 293–311.
15. Ellwood, B. B. and Ledbetter, M. T., *Earth Planet. Sci. Lett.*, 1977, **35**, 189–198.
16. Dvorak, J. and Hrouda, F., in *The Magnetic Anisotropy of Rocks* (eds Tarling, D. H. and Hrouda, F.), Chapman and Hall, London, 1975.
17. Srivastava, J. P., Verma, S. N., Joshi, V. K., Verma, B. C. and Arora, R. K., *Geol. Surv. India, Sp. Publ.*, 1988, **11/2**, 233–241.
18. Marshak, S. and Mitra, G., *Basic Methods of Structural Geology*, Prentice Hall, NJ, 1988, pp. 145–174.

ACKNOWLEDGEMENTS. We thank the Director, Wadia Institute of Himalayan Geology, Dehra Dun for providing the necessary facilities and support. Mr Rakesh Kumar is acknowledged for his assistance during sampling and analysis.

Received 29 September 2000; revised accepted 29 March 2001